Atmospheric Environment 161 (2017) 1–12

Contents lists available at ScienceDirect

Atmospheric Environment

journal homepage: www.elsevier.com/locate/atmosenv

Characterizations of volatile organic compounds (VOCs) from vehicular emissions at roadside environment: The first comprehensive study in Northwestern China

Bowei Li [a, b], Steven Sai Hang Ho [a, c, d], Yonggang Xue [a, c], Yu Huang [a, c, *], Liqin Wang [a, c], Yan Cheng [b], Wenting Dai [a, c], Haobin Zhong [a, c], Junji Cao [a, c], Shuncheng Lee [e]

[a] Key Lab of Aerosol Chemistry & Physics, Institute of Earth Environment, Chinese Academy of Sciences, Xi'an 710061, China
[b] Department of Environmental Science and Technology, School of Human Settlements and Civil Engineering, Xi'an Jiaotong University, Xi'an 710049, China
[c] State Key Lab of Loess and Quaternary Geology (SKLLQG), Institute of Earth Environment, Chinese Academy of Sciences, Xi'an 710061, China
[d] Division of Atmospheric Sciences, Desert Research Institute, Reno, NV, USA
[e] Department of Civil and Environmental Engineering, The Hong Kong Polytechnic University, Hung Hom, Hong Kong

HIGHLIGHTS

- VOCs have been quantified at a roadside environment in Xi'an, China first time.
- Isopentane was the most abundant compound in the traffic-dominated environment.
- Different vehicular sources were resolved by a receptor model.
- Compressed natural gas (CNG) combustion has a distinct impact on ozone formation.

GRAPHICAL ABSTRACT

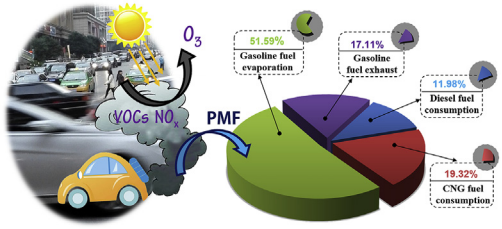

ARTICLE INFO

Article history:
Received 30 December 2016
Received in revised form
18 April 2017
Accepted 20 April 2017
Available online 22 April 2017

Keywords:
VOCs
Ozone precursors
Roadside
Vehicular emissions
Source apportionment

ABSTRACT

Vehicular emission (VE) is one of the important anthropogenic sources for ground-level volatile organic compounds (VOCs) in both urban and suburban areas. A first comprehensive campaign was conducted at an urban roadside in Xi'an, China in summer, 2016. A total of 57 VOCs, as known as critical surface ozone (O_3) precursors, and other trace gases were measured simultaneously during the sampling period. *Iso*-pentane, a tracer of gasoline evaporation, was the most abundant VOC in the roadside samples, followed by isobutane and benzene, attributed to the largest composition (~70%) of gasoline-fueled vehicles on the road. The molar ratio of toluene/benzene (T/B) in our study (0.36) is far lower than the range reported in other cities, indicating the stronger contributions from diesel emissions. The results of source apportionment achieved with positive matrix factorization (PMF) receptor model were highly consistent with the vehicles compositions, strongly evidenced that the precise characterization of the VE sources from those marker species. The degrees of individual compound contributed to O_3 production were weighed by ozone formation potential (OFP). Propylene (20%), 1-butene (11%) and *iso*-pentane(10%) were the top three contributors at the roadside. The information of this study complements the VOCs database regarding to the VE sources in Northwestern China.

* Corresponding author. Key Lab of Aerosol Chemistry & Physics, Institute of Earth Environment, Chinese Academy of Sciences, Xi'an 710061, China.
E-mail address: huangyu@ieecas.cn (Y. Huang).

http://dx.doi.org/10.1016/j.atmosenv.2017.04.029
1352-2310/

1. Introduction

Volatile organic compounds (VOCs) are known ingredients in the photochemical production of tropospheric ozone (O_3) in the presence of nitrogen oxides (NO_x) and sunlight. They are actively contributed in formation of secondary organic aerosol (SOA) through a chain of photochemical reactions and consequent gas-to-particle condensations (Finlayson-Pitts and Pitts, 1997; Atkinson, 2000; Jenkin and Clemitshaw, 2000; Andersson-Sköld and Simpson, 2001; Kansal, 2009; Ning and Sioutas, 2010; Ziemann and Atkinson, 2012). The Photochemical Assessment Monitoring Stations (PAMS) organized by United States Environmental Protection Agency (U.S.EPA) has particularly defined 57 critical ozone precursors ($VOCs_{PAMS}$) (Shao et al., 2016). Several of these such as benzene, toluene, and 1,3-butadienehave been evidenced to be air toxics for their adverse effects on human health, including nose and throat irritation, asthma and leukemia, and even death (Knox, 2005; Kampa and Castanas, 2008; Wang et al., 2016).

Vehicular emission (VE) is one of the most important pollution sources for anthropogenic VOCs in urban and suburban areas in China (Guo et al., 2004; Velasco et al., 2007; Liu et al., 2008b; Lyu et al., 2016; Wu et al., 2016a; 2016b). Liu et al. (2008b) reported that VE contributed >50% to the ambient VOCs at urban Guangzhou, while the contribution of VE to the overall atmospheric VOCs was as high as 65 ± 36% in Hong Kong (Guo et al., 2007). Acquisition and interpretation of its source profile are particularly critical for remediation of the severe air pollution. Driving condition, class, age and millage of engine, fossil fuel composition, and catalyst-equipped in pollutant-removal system can significantly vary the chemical compositions of VE (Ho et al., 2013; Chiang et al., 2007; Wang et al., 2013). Unfavorable meteorological conditions can cause pollutant accumulation. Under poor atmospheric dispersion, distinctly high levels of monocyclic aromatic hydrocarbons (i.e., benzene and toluene) were measured in a heavy traffic area in Nanjing, where unleaded fuels were used in major (Wang and Zhao, 2008).

Most of current Chinese traffic-related VOCs researches were conducted in Beijing-Tianjin-Hebei (JJJ), Yangtze River Delta (YRD) and Pearl River Delta (PRD) regions (Wang and Zhao, 2008; Ho et al., 2013; Huang et al., 2015), while neither report and databases are available in northwestern regions. Xi'an is a popular and traditional tourist destination in China and even the world. It has an over 8 million population and is under rapid economic growth (Feng et al., 2016). The city is thus considered as a representative to northwestern China. Heavy air pollution events like haze and photochemical smog have frequently occurred in Xi'an and its surrounding areas owing to increase of local anthropogenic emissions, regional pollutants transportation, and poor air dispersion (Cao et al., 2011; Wang et al., 2012a; Feng et al., 2016). According to the statistic, the numbers of registered motor-vehicles have rapidly increased from ~180,000 in 1997 to >2,500,000 in 2016 (Song, 2016). Even though the vehicle number was 30–70% lower, the VE contribution was ~2.7–4.0 times the levels in other Chinese megacities (i.e., as Beijing, Shanghai and Guangzhou) (Huang et al., 2014). A less stringent local vehicle emission standard might be an explanation to the case. In addition, great variations on both vehicle types and fuel compositions can be found between those cities. For vehicles, implementation of restrict engine emission standards in Beijing, Shanghai, Guangzhou are often faster than that in other sub-national regions due to differentiate rates of capitalization and policy executions. For fuel, compositions of gasoline and diesel supplied to those regions were also differentiated (Li, 2016). Small constituent changes could lead a certain degree differences on pollutant formation from the engines. These factors caused variations on emission profile among the sub-national regions.

The objective of this study is to acquire the VOC_{PAMS} profile at a roadside in urban Xi'an. Correlations between the VOCs species and vehicle types have been interpreted with the potential source markers of fuels and receptor models. Temporal variations of the chemical species were also obtained. Chemical reactivity of VOC_{PAMS} was evaluated by means of calculating their ozone formation potential (OFP). The findings are critical to complement the database in northwestern China.

2. Methodology

2.1. Sampling site

The sampling location is an interception point between two main roads, Yanxiang Road and Xingqing Road, where located under the Shapo Overpass of the South Secondary Ring Road in Beilin District, Xi'an (Fig. 1). It represented as a heavy daily traffic environment in the city. The site was close to few commercials (~50 m) and residential buildings (>100 m), and their heights were all below 10 m. No other obvious emission source rather than VE was identified nearby from routine inspections during the sampling campaign.

2.2. Sample collection

The sampling campaign was conducted between May 19th and June 6th, 2016. Selection of study period is based on fact that higher ambient O_3 concentrations are generally observed in summer than other seasons. It is thus more informative to investigate the contribution of VOC emissions from vehicles to the atmospheric O_3. Besides, more frequently short-term and sudden rains would occur in late summer (i.e., July–August), which cause unsuitable conditions for the sampling. In the first section (from May 19th to June 3rd, 2016), offline time-integrated VOCs samples were collected and real-time data for trace gases, including carbon monoxide (CO), carbon dioxide (CO_2), nitrogen dioxide (NO_2)/NO_x, and O_3, were recorded simultaneously in four different sampling time intervals of (I) 07:00–09:00, (II) 12:00–14:00, (III) 18:00–20:00, and (IV) 00:00–02:00.

The VOCs in the air was drawn into a ¼" o.d. stainless steel multi-bed adsorbent tube filled with Tenax-TA, Carbograph I TD and Carboxen 1003 (C3-DXXX-5266, ca. 380 mg in adsorbent weight per tube, Markes International Ltd., Llantrisant, U.K.) using a low-flow module pump (ACTI-VOC, Markes International Ltd.) at a flow rate of 50 mL min^{-1} for 60 min (i.e., total sampling volume = 3 L). Insignificant breakthrough (<5%) was observed either in field or laboratory demonstration under this sampling flow and volume (Ho et al., 2017). Two sorbent tube samples were thus collected in each time interval. The sampling inlet was set-up at 1.5 m above the ground level. Prior to the sampling, all sorbent tubes were cleaned in a thermal conditioner (TC20, Markes International Ltd.) at 330 °C for 20 min before use. All pre-conditioned and sampled tubes were sealed with Difflok caps (Markes International Ltd.) and stored in desiccators at 0 °C for a maximum of two weeks. The desiccators were filled with silica gel and activated carbon to avoid passive absorption of any water vapor and VOCs, respectively. The pump was calibrated with a mass flow calibrator (Defender 510, Bios, Torrance, CA, USA) before each sampling event. A Teflon filter assembly (47 mm, Whatman, Clifton, NJ, USA) and a home-made ozone scrubber, manufactured by a 1 m long and ¼" o.d. saturated potassium iodide (KI) coated copper tube, were installed in the air upstream to remove any influences from particulate matter (PM) and O_3, respectively. The O_3 removal efficiency was >99% at a concentration level of 100 ppbv for 60 min in laboratory test. One field blank was collected on each sampling day.

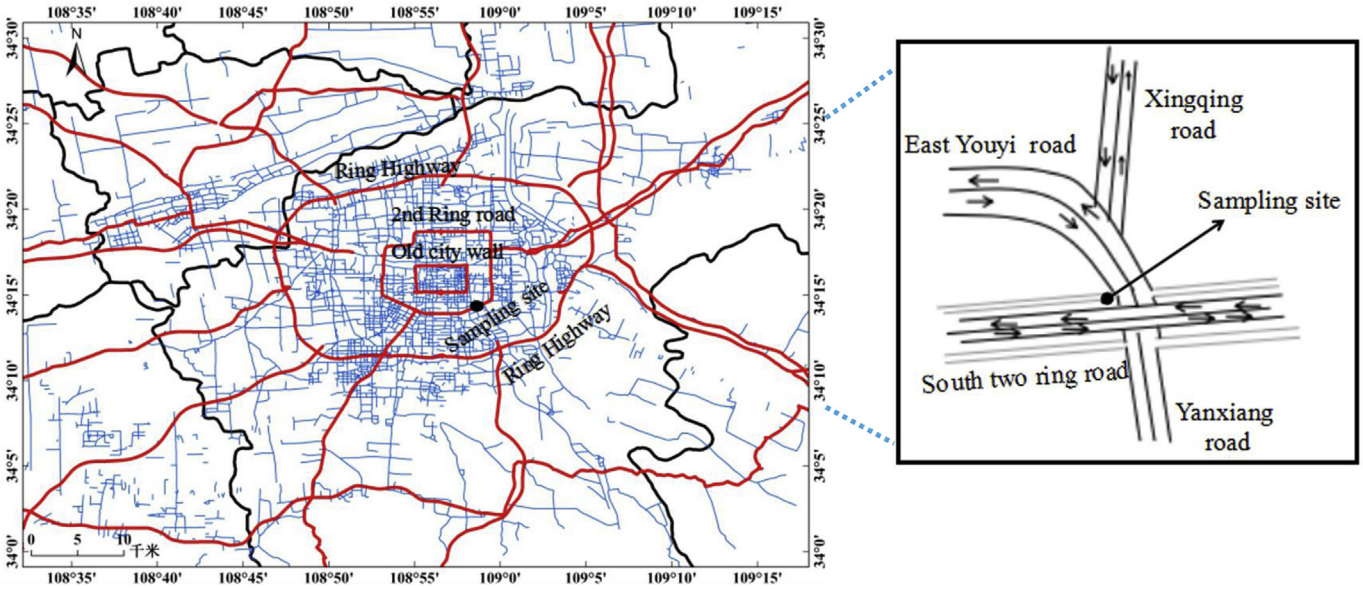

Fig. 1. Map of the sampling location and road conditions in Xi'an.

The sorbent samples were properly transported to the laboratory for chemical analysis.

Real-time concentrations of the trace gases were monitored continuously during the sampling event. The CO was measured by a non-dispersive infrared (NDIR) photometer (EC9810, Ecotech, Blackburn, Australia), NO_2/NO_x was measured by chemiluminescence detector (Model 42i, Thermo Electron, Waltham, MA, USA), and O_3 was monitored by an ultra-violet (UV) photometric O_3 analyzer (EC9810, Ecotech). All sampling equipments were all set up at 1.5 m above the ground level. The time resolution for these instruments was 5 min and the minimum detection limit (MDL) were 0.05 ppmv for CO, 0.5 ppbv for NO_2/NO_x, and 0.5 ppbv for O_3.

The second section of the campaign consisted of intensive samplings, which were conducted for three consecutive days from June 3rd to June 6th, 2016. One sorbent tube sample for the VOCs measurement was collected bi-hourly. A total of 12 samples were thus taken per day. The real-time concentrations for the trace gases were monitored simultaneously.

2.3. Traffic number count and vehicle type

Traffic numbers were obtained by setting two video cameras to record the road condition. The videos were downloaded into computer every 24 h and reviewed by an operator. The relevant vehicle types were also classified with the operator's inspection, including (1) gasoline-fueled private cars; (2) compressed natural gas (CNG)-fueled taxis; (3) CNG-fueled public buses; (4) diesel-fueled light-duty vehicles; and (5) diesel-fueled heavy-duty vehicles. The differences on traffic number counts and vehicle type classification conducted by two operators were <10%. Due to limitations in realistic environment, traffic speeds and age and millage of engines could not be obtained in this study.

2.4. VOCs analysis with TD-GC/MS method

A total of 145 valid sorbent tube samples were collected. They were all analyzed using a thermal desorption (TD) unit (Series 2 UNITY-xr system, Markes International Ltd.) coupled with a gas chromatograph/mass spectrometric detector (GC/MSD, Models 7890A/5977 B, Agilent, Santa Clara, CA, USA) within one week. A tube was connected into the TD unit at room temperature (~25 °C) and purged with ultra-high purity (UHP) helium (He) gas at a flow rate of 40 mL min^{-1} for 10 s to eliminate air and oxygen intrusion. For the primary desorption stage, the analytes were desorbed at 330 °C for 5 min and refocused onto a cryogenic-trap (U-T1703P-2S, Markes International Ltd.) to capture high volatility target compounds at −15 °C. For the secondary desorption stage, the trap was dry-purged for 10 s and rapidly heated from −15 °C to 320 °C and maintained for 5 min. The analytes were passed via a heated transfer line at 160 °C, and re-refocused onto a cold GC capillary column head (Rtx®-1, 105 m × 0.25 mm × 1 μm film thickness, Restek Corporation, Bellefonte, PA, USA) at −45 °C with an aid of liquid nitrogen (N_2) in GC oven. Once the second desorption is completed, the oven temperature program started at an initial temperature of −45 °C for 4 min, ramped to 230 °C at a rate of 6 °C min^{-1}, and maintained at 230 °C for 5 min. The constant flow rate of He carrier gas was 1.0 mL min^{-1} throughout the GC analysis. The MSD was operated in selective ion monitoring (SIM) mode at 230 °C and 70 eV for electron ionization. Identification was achieved by comparing the mass spectra and retention times of the chromatographic peaks with those authentic standards. Certified PAMS standard mixtures (Restek Corporation) were used in calibrations. A multi-point calibration curve was established to quantify each of the target compounds with linearity>0.999. The minimum detection limits (MDL) were in the range of 0.003–0.808 ppbv with a sampling volume of 3 L (Table 1). The measurement precision for the analysis of eight replicates of standard samples at 2 ppbv were ≤5%.

2.5. Positive matrix factorization (PMF) receptor model

Positive matrix factorization (PMF) is an efficient factor analysis model, from which an analyst can extract representative sources and specific contributions of each source by means of decomposing one matrix into two, and it has been widely used around the world for identifying major sources of PM and VOCs without any knowledge of emission profiles at first. Comparisons between PMF and another source apportionment model chemical mass balance (CMB) demonstrate that PMF have a better performance in

Table 1
Mixing ratios of trace gases and $VOCs_{PAMS}$ and the numbers of vehicle counts at roadside.

	MDL	I 07:00–09:00		II 12:00–14:00		III 18:00–20:00		IV 00:00–02:00		Average	
		Mean	SD	Mean	SD	Mean	SD	Mean	SD	Mean	SD
Trace gases											
CO (ppmv)	0.05	2.40	0.32	2.22	0.29	2.46	0.30	2.02	0.37	2.27	0.20
O_3 (ppbv)	0.5	6.61	6.40	29.75	17.65	18.47	10.66	21.53	18.60	19.09	9.58
NO (ppbv)	0.5	90.53	39.69	36.05	17.90	65.47	31.04	19.82	23.60	52.97	31.37
NO_2 (ppbv)	0.5	32.48	7.15	39.58	10.89	53.89	13.82	24.58	12.48	37.63	12.45
Alkanes (ppbv)											
Ethane	0.40	0.85	0.44	0.63	0.29	0.89	0.51	0.55	0.39	0.69	0.43
Propane	0.21	1.97	0.85	2.09	0.87	2.28	0.83	2.06	1.28	1.84	0.95
Isobutane	3.47	9.06	8.67	6.34	5.11	7.36	8.23	7.55	5.85	7.69	7.17
n-Butane	0.20	2.33	0.96	2.02	0.73	2.29	0.55	1.76	0.94	2.00	0.80
iso-Pentane	0.08	12.09	5.28	13.49	10.21	15.44	10.90	10.58	6.51	11.63	7.88
n-Pentane	0.10	1.62	0.74	1.48	0.62	1.64	0.64	1.20	0.80	1.41	0.66
2,2-Dimethylbutane	0.15	bd[a]	bd	bd	bd	bd	bd	Bd	bd	bd	bd
Cyclopentane	0.16	5.37	4.73	16.40	18.53	1.25	1.05	2.29	3.74	4.81	9.48
2,3-Dimethylbutane	0.09	0.23	0.08	0.27	0.28	0.24	0.10	0.18	0.09	0.22	0.14
2-Methylpentane	0.11	0.87	0.54	0.87	0.54	0.93	0.48	0.73	0.51	0.83	0.50
3-Methylpentane	0.09	0.56	0.40	0.55	0.41	0.57	0.36	0.48	0.40	0.53	0.38
n-Hexane	0.03	2.37	3.73	2.54	3.94	2.32	3.30	2.34	3.20	2.38	3.44
Methylcyclopentane	0.08	0.31	0.16	0.28	0.18	0.30	0.15	0.29	0.17	0.28	0.16
2,4-Dimethylpentane	0.09	0.09	0.00	0.18	0.12	0.12	0.03	0.05	bd	0.12	0.07
Cyclohexane	0.09	0.48	0.45	0.51	0.50	0.50	0.44	0.67	0.36	0.54	0.42
2-Methylhexane	0.12	0.37	0.13	0.40	0.19	0.44	0.24	0.29	0.13	0.36	0.18
2,3-Dimethylpentane	0.34	bd	bd	bd	bd	bd	bd	Bd	bd	bd	bd
3-Methylhexane	0.12	0.26	0.08	0.27	0.13	0.29	0.13	0.21	0.06	0.24	0.11
2,2,4-Trimethylpentane	0.17	0.20	bd	0.21	0.05	0.23	0.05	0.13	0.07	0.20	0.06
n-Heptane	0.12	0.35	0.27	0.33	0.20	0.34	0.22	0.32	0.25	0.38	0.28
Methylcyclohexane	0.09	0.13	0.04	0.13	0.06	0.14	0.05	0.13	0.01	0.13	0.04
2,3,4-Trimethylpentane	0.12	bd	bd	bd	bd	0.13	bd	Bd	bd	0.13	bd
2-Methylheptane	0.11	bd	bd	0.14	0.03	0.16	0.05	0.13	bd	0.14	0.04
3-Methylheptane	0.22	bd	bd	bd	bd	bd	bd	Bd	bd	bd	bd
n-Octane	0.15	0.17	0.03	0.17	0.02	0.18	0.03	0.15	0.02	0.17	0.03
n-Nonane	0.12	0.29	bd	0.14	0.04	0.16	0.04	0.14	0.00	0.16	0.05
n-Decane	0.04	0.15	0.14	0.21	0.34	0.15	0.11	0.17	0.20	0.14	0.19
Undecane	0.03	0.28	0.26	0.25	0.18	0.28	0.16	0.43	0.77	0.24	0.36
Dodecane	0.09	0.77	0.46	0.89	1.54	0.73	0.47	1.39	3.16	0.76	1.49
Sum of alkanes		*30.57*	*14.39*	*29.56*	*19.33*	*31.91*	*16.83*	*25.82*	*11.20*	*26.41*	*14.81*
Alkenes (ppbv)											
Ethylene	2.03	2.24	1.98	1.79	1.39	2.81	3.75	2.00	3.21	1.99	2.60
Propylene	1.88	3.37	0.87	3.40	2.01	4.16	2.13	3.28	1.83	3.38	1.68
1-Butene	1.43	2.70	1.80	1.62	0.14	1.78	0.35	1.49	bd	1.95	0.80
trans-2-Butene	0.24	0.36	0.09	0.35	0.12	0.42	0.19	0.32	0.10	0.36	0.13
cis-2-Butene	0.20	0.28	0.07	0.28	0.08	0.32	0.11	0.25	0.05	0.28	0.09
1-Pentene	0.14	0.29	0.12	0.59	1.30	0.32	0.12	0.24	0.10	0.34	0.57
Isoprene	0.30	0.46	0.16	0.54	0.15	0.57	0.27	0.31	0.02	0.50	0.18
trans-2-Pentene	0.13	0.25	0.07	0.24	0.10	0.27	0.10	0.18	0.08	0.23	0.09
cis-2-Pentene	0.12	0.16	0.03	0.16	0.04	0.18	0.05	0.16	0.04	0.17	0.04
1-Hexene	0.11	0.18	0.12	0.16	0.07	0.18	0.09	0.13	0.06	0.15	0.09
Sum of alkene		*6.12*	*3.50*	*5.79*	*4.44*	*7.78*	*6.18*	*5.35*	*4.89*	*5.40*	*4.55*
Aromatics (ppbv)											
Benzene	0.84	3.90	1.54	4.67	2.96	4.95	2.78	3.14	1.84	3.75	2.31
Toluene	0.22	1.56	0.69	1.41	0.99	1.62	1.02	1.04	0.57	1.33	0.83
Ethylbenzene	0.09	0.31	0.11	0.34	0.18	0.39	0.22	0.26	0.13	0.30	0.17
m,p-Xylene[b]	0.08	0.85	0.27	0.88	0.45	1.16	0.72	0.69	0.39	0.82	0.50
Styrene	0.04	0.16	0.11	0.19	0.17	0.23	0.18	0.17	0.16	0.16	0.15
o-Xylene	0.07	0.29	0.09	0.34	0.22	0.41	0.25	0.25	0.14	0.29	0.19
Isopropylbenzene	0.05	0.08	0.02	0.13	0.09	0.11	0.07	0.10	0.03	0.11	0.07
n-Propylbenzene	0.04	0.07	0.03	0.09	0.08	0.09	0.07	0.06	0.05	0.07	0.06
m-Ethyltoluene	0.04	0.14	0.05	0.18	0.15	0.21	0.13	0.13	0.09	0.15	0.11
p-Ethyltoluene	0.02	0.08	0.03	0.12	0.11	0.13	0.08	0.08	0.06	0.09	0.07
1,3,5-Trimethylbenzene	0.03	0.11	0.06	0.15	0.20	0.16	0.13	0.10	0.10	0.11	0.12
o-Ethyltoluene	0.03	0.11	0.05	0.15	0.17	0.16	0.13	0.10	0.09	0.11	0.11
1,2,4-Trimethylbenzene	0.04	0.33	0.12	0.45	0.35	0.51	0.31	0.32	0.23	0.35	0.26
1,2,3-Trimethylbenzene	0.03	0.17	0.09	0.23	0.25	0.26	0.20	0.19	0.19	0.18	0.18
m-Diethylbenzene	0.02	0.10	0.07	0.11	0.15	0.12	0.11	0.10	0.10	0.09	0.10
p-Diethylbenzene	0.02	0.13	0.07	0.16	0.15	0.19	0.12	0.14	0.13	0.13	0.11
Sum of aromatics		*8.32*	*2.84*	*9.33*	*5.32*	*10.63*	*5.62*	*6.79*	*3.51*	*7.90*	*4.46*
$TVOCs_{PAMS}$		**45.01**	**18.89**	**44.68**	**27.05**	**50.31**	**26.77**	**37.97**	**17.90**	**39.71**	**22.03**
Vehicles											
Gasoline-fueled vehicle		7158	1696	6666	1085	8460	1112	1166	383	6014	2968

Table 1 (*continued*)

	MDL	I 07:00–09:00		II 12:00–14:00		III 18:00–20:00		IV 00:00–02:00		Average	
		Mean	SD	Mean	SD	Mean	SD	Mean	SD	Mean	SD
CNG-fueled taxi		1008	454	1272	262	954	198	1275	344	1123	345
CNG-fueled bus		1044	177	942	92	924	140	27	54	757	421
Diesel-fueled HD[c]		96	63	192	68	102	31	123	127	129	83
Diesel fueled LD[d]		390	233	690	207	402	109	55	105	395	279
Sum of vehicles		*9696*	*2623*	*9762*	*1714*	*10 842*	*1589*	*2647*	*1013*	*8417*	*3424*

[a] bd represents below MDL.
[b] *m*-Xylene and *p*-xylene are co-eluted in the chromatographic separation.
[c] HD stands for heavy duty.
[d] LD stands for light duty.

extracting major sources from similar database (Miller et al., 2002), and any negative contributions will be excluded in PMF model run. In this study, EPA PMF3.0 receptor model was applied to distinguish dominant sources at the roadside environment.

The PMF model can be expressed as a chemical mass balance equation in terms of contributions from p independent sources to n chemical species measured in a given sample (Miller et al., 1972):

$$x_{ij} = \sum_{k=1}^{p} g_{ik} f_{kj} + e_{ij} \quad (1)$$

where x_{ij} is the jth chemical species concentration determined in the ith sample, g_{ik} is the species contribution of the kth source to the ith sample, f_{kj} is the loading of jth species on the kth factor, e_{ij} is the residual resulting from bias in the measurement of g_{ik} and f_{kj}, and p represent the total number of independent sources (Paatero, 1997).Every data point can be individually weighed in PMF, so that the retainment of data below detection limit with its associated uncertainty was permissible. Analysts can evaluate the stability of the solution by means of examining the proportion of each source undertaken in terms of the object function Q:

$$Q = \sum_{t=1}^{n} \sum_{j=1}^{m} \left[\frac{x_{ij} - \sum_{k=1}^{p} g_{ik} f_{kj}}{\mu_{ij}} \right]^2 \quad (2)$$

Where μ_{ij} represents the uncertainty of jth species in ith sample.

For the PMF input, the uncertainty caused by sampling and analytical errors was calculated using the following equation suggested by Polissar et al. (1998):

$$U = \sqrt{(EF \times conc)^2 + (MDL)^2} (conc > MDL) \partial \quad (3)$$

Where EF represent the error fraction, which is the result of the relative standard deviations of the instrument multiply 100, and we set it as 0.02, equal to the average percent uncertainty in our study. For values below detection limit, the uncertainties were replaced by 5/6 times of the detection limit values. Missing data are replaced with the median concentration of that species and the uncertainty are expressed as four times the median concentration (USEPA, 2008).

3. Results and discussions

3.1. Sampling time selection

Sampling time selection was based on the traffic number counts and meteorological conditions. In the weekdays, the highest traffic frequencies were often recorded in our three daytime intervals (i.e., I, II, and III), which are corresponding to pre-on-duty/school (07:00–09:00), lunch (12:00–14:00), and post-off-duty/school periods (18:00–20:00), respectively. Solar energy was the strongest around the noon time (II). The lowest traffic frequencies were counted in the night interval of IV (00:00–02:00) but with different vehicle compositions, appointing to a comparison to the daytimes. Neither the traffic number counts nor vehicle types did not show statistically differences ($p < 0.05$) between the weekdays and weekends, even for time intervals of I and III, potentially attributed to residents' usual outgoing practice for entertainment or travelling in the morning and homing in the evening, respectively, in non-working days.

3.2. VOCs levels and compositions

Mixing ratios of the 57 $VOCs_{PAMS}$ and traces gases in the first section of sampling campaign were summarized on Table 1. The mixing ratio of total quantified VOCs ($TVOC_{PAMS}$) ranged from 11.5 to 101.4 ppbv (39.71 ± 22.03 ppbv on average). Acetylene is the only alkyne in the list but its mixing ratios in the samples were all below the MDL. The lowest $TVOC_{PAMS}$ (37.97 ± 17.90 ppbv on average) were seen in the night interval of IV, consistent with the fewest numbers of vehicles (i.e., >30% of the daytime values) across the sampling site. The most abundant VOC in the roadside samples was *iso*-pentane, followed by *iso*-butane and benzene, with the average mixing ratios of 11.63 ± 7.88, 7.69 ± 7.17, and 3.75 ± 2.31 ppbv, respectively. Table S1 compares the mixing ratios of 25 representative $VOCs_{PAMS}$ quantified in roadside environments in Beijing, Hong Kong, and Tokyo (Hoshi et al., 2008; Li et al., 2015; Huang et al., 2015). The average sum of these $VOCs_{PAMS}$ in Xi'an (46.51 ppbv) was higher than those in Tokyo (27.4 ppbv), Hong Kong (39.8 ppbv) and Beijing (39.9 ppbv). It must be noted that the absolute abundances can be strongly impacted by local traffic frequencies and both of geographical and meteorological conditions at the sampling sites. The higher VOCs mixing ratios can be ascribed to a heavier traffic with less dispersion at our site during the sampling periods. The wind speed measured at 3 m height was 0.62 ± 0.70 m s^{-1} on average (Table 2), which was much lower than those of 4.19–7.50 m s^{-1} and 3.86–6.85 m s^{-1} in Hong Kong (Huang et al., 2015) and Beijing (Li et al., 2015), respectively. The wind speeds could drastically change depending on the measurement height. The low air mass dispersion can be ascribed to covering from the surrounding buildings and all sampling equipment were setup at 1.5 m above the ground level.

Chemical compositions of the roadside samples more efficiently reflect the traffic patterns. Fig. 2 illustrates the average $VOCs_{PAMS}$ profiles in the four time intervals. Alkanes was the most abundant organic class in both daytime and nighttime, ranging from a molar ratio of 61–71% of the $TVOC_{PAMS}$, followed by aromatics (21–24%) and alkenes (12–14%). *Iso*-pentane had the highest contribution of 28.5 ± 10.2% which is an important component in gasoline and acts

Table 2
Wind speeds measured at the sampling site.

Height of wind speed measurement (m)	Wind speed (m/s)		Horizontal wind (m/s)		Cross-sectional wind (m/s)	
	variation range	Average	variation range	Average	variation range	Average
3	0–3.4	0.62 ± 0.70	0–2.6	0.24 ± 0.34	0–4.3	0.52 ± 0.66

as a marker for gasoline evaporation (Han et al., 2015). Benzene, toluene, ethylbenzene, *m*,*p*-xylene, with an abbreviation as BTEX, had a sum of contribution of 16.9 ± 7.0% to the $TVOC_{PAMS}$. BTEX are the most abundant aromatic compounds in urban areas which are considered to be emitted from VE-related sources in major (Wang et al., 2012b; Zhang et al., 2012).

Fig. S1 compares the compositions of those marker species with other studies. The contributions of ethane, propane, *n*-butane and *iso*-butane were much higher in Beijing and Hong Kong than those in Xi'an due to the differences in fuels consumption and compositions (Li et al., 2015; Huang et al., 2015). Propane (26.0%), *n*-butane (46.4%) and *iso*-butane (22.4%) are the three major liquefied petroleum gas (LPG) constituents in Hong Kong (Tsai et al., 2006), where >99% of public mini-buses and taxis are currently LPG-fueled. The three alkanes were thus the most abundant VOCs collected in the Hong Kong roadside samples (Huang et al., 2015). No LPG-fueled vehicles were found in Xi'an instead. Besides, the high compositions of ethane can be attributed to more transportation-related (i.e., industrial) and LPG and CNG emissions in Beijing (Wang et al., 2015). Local emission standards executed, fuel compositions, and dominances of vehicles types can greatly influence the VOCs profiles at the roadside environments.

3.3. Correlations between VOCs and vehicle compositions

Local vehicles were mainly fueled with CNG, gasoline, or diesel in Xi'an. Motorcycles were charged by electricity with no direct emissions, thus were excluded in the statistic. The traffic counts at the four time intervals were generally stable between each sampling day, with a small peak observed in the evening (III). Fig. 3 presents the variations of traffic counts and $TVOC_{PAMS}$ in a selective period from May 27th to May 30th. Their consistent trend demonstrates the positive relationship between the mixing ratios and traffic frequencies at the roadside. The maximum and minimum of $TVOC_{PAMS}$ were measured in the evening (III) and night (IV), respectively, which also agreed with the traffic counts.

The sum of the common VE markers including ethane, propane, *iso*-butane, *n*-butane, *iso*-pentane, *n*-C_9-C_{12} alkane, ethylene, isoprene, benzene, and toluene contributed >60% of the $TVOC_{PAMS}$. Those VOCs had intimate relationship with VE, and their emission characters should be more sensitive to the variations of vehicle compositions in contrast to other species. Based on our statistic, the gasoline-fueled private cars contributed 69–79% to the total number of vehicle counts in the day intervals. No significant variations (≤10%) on vehicles type compositions were found among the three intervals, additionally supporting with their relatively stable $VOCs_{PAMS}$ profiles (Fig. 2).

The highest composition of CNG-fueled vehicles of 49 ± 8% was often found in the night interval (IV), compared to <20% in the daytimes. Methane (~90%), propane (1–6%) and propene (0.2–2%) are the three major VOC constituents in the CNG provided in Xi'an (Yun, 2015). Liu et al. (2008a) reported that the combustion of CNG emitted propane and *n*-butane in major. The CNG evaporation could not be evaluated as methane (CH_4) was not included in the measurement. Distinctly higher molar compositions of longer chain alkanes (C_9-C_{12}, including *n*-nonane,*n*-decane, undecane, dodecane) (1.5–7.5%) were found in the night interval as well, attributed to the larger proportion of diesel-fueled vehicles (9.6 ± 11.7%) for general practice of goods transportation. Besides, isoprene is a major tracer of biogenic emissions with high reactivity, but VE could be a potential source as well (Lu et al., 2007; Araizaga et al., 2013). Araizaga et al. (2013) reported that the emission factors for isoprene ranged from 1.02 ± 1.12 to 1.63 ± 0.10 mgkm-veh^{-1} under different driving conditions in a tunnel study, even though an opposite trend was observed between the mixing ratio of isoprene and the vehicle numbers in an urban atmosphere in Beijing (Wang et al., 2015).

3.4. Temporal variation

The three-days strengthen sampling further demonstrated that the relationship between the mixing ratios of $VOCs_{PAMS}$, trace gases, and traffic frequencies (Fig. 4). From 07:00 on June 2 to 09:00 on June 3, medium rains occurred. Lower mixing ratios of O_3 were measured in comparison with the levels at corresponding times in other sampling dates. With consistent traffic numbers, the direct-emission trace gases of $VOCs_{PAMS}$, CO, NO and NO_2 did not show any decline since they were resistant to be washed out. Most importantly, the rain would help prevent O_3 from forming while dry weather increases O_3 formation. Without raining, higher mixing ratios of $VOCs_{PAMS}$ were detected in noon and evening intervals, coincided with the larger traffic volumes. Among the daytimes, lower $TVOC_{PAMS}$ levels were measured in the early morning even though high traffic numbers were recorded around the pre-on-duty/school times (i.e., 07:00–09:00). This can be resulted from less accumulation of polluted airs from the lower emissions from VE during the night.

3.5. Correlations between VOCs species

Iso-pentane is one of the most abundant VOC in the traffic-related sources (Liu et al., 2008a; Lai and Peng, 2012; Wang et al., 2015), but sparsely generated from other pollution origins such as industrial, solvent usage and biomass burning (Wang et al., 2014; Liu et al., 2008a). It is consequently considered as an effective reference to evaluate the significance of a given compound to VE by their correlations. In this study, excellent correlations between *iso*-pentane/benzene (0.90) and *iso*-pentane/toluene (0.87) were demonstrated (Fig. 5). And the correlation between benzene and toluene (0.85) was a bit higher than that reported in other studies. Buczynska et al. (2009) determined the correlation coefficient of 0.83 for benzene and toluene at an intensive traffic region in Antwerp, Belgium, while Wang et al. (2002) calculated the value of 0.77 at a roadside site in urban Macau, China. These illustrate that the formations of benzene and toluene from VE could be different due to a variety of fuels or engines in Xi'an.

Table 3 compares the mixing ratios of BTEX measured in different traffic-impacted environments. It is obvious that much higher benzene (3.91 ± 2.70 ppbv) but lower toluene (0.80 ± 0.47 ppbv) mixing ratios were measured in Xi'an. With calculation of the molar ratio of toluene/benzene (T/B), our value of 0.36 is far lower than the range of 1.77–3.22 reported in north-eastern and southern China and other cities. Such difference could be ascribed to the stronger contributions from diesel emissions,

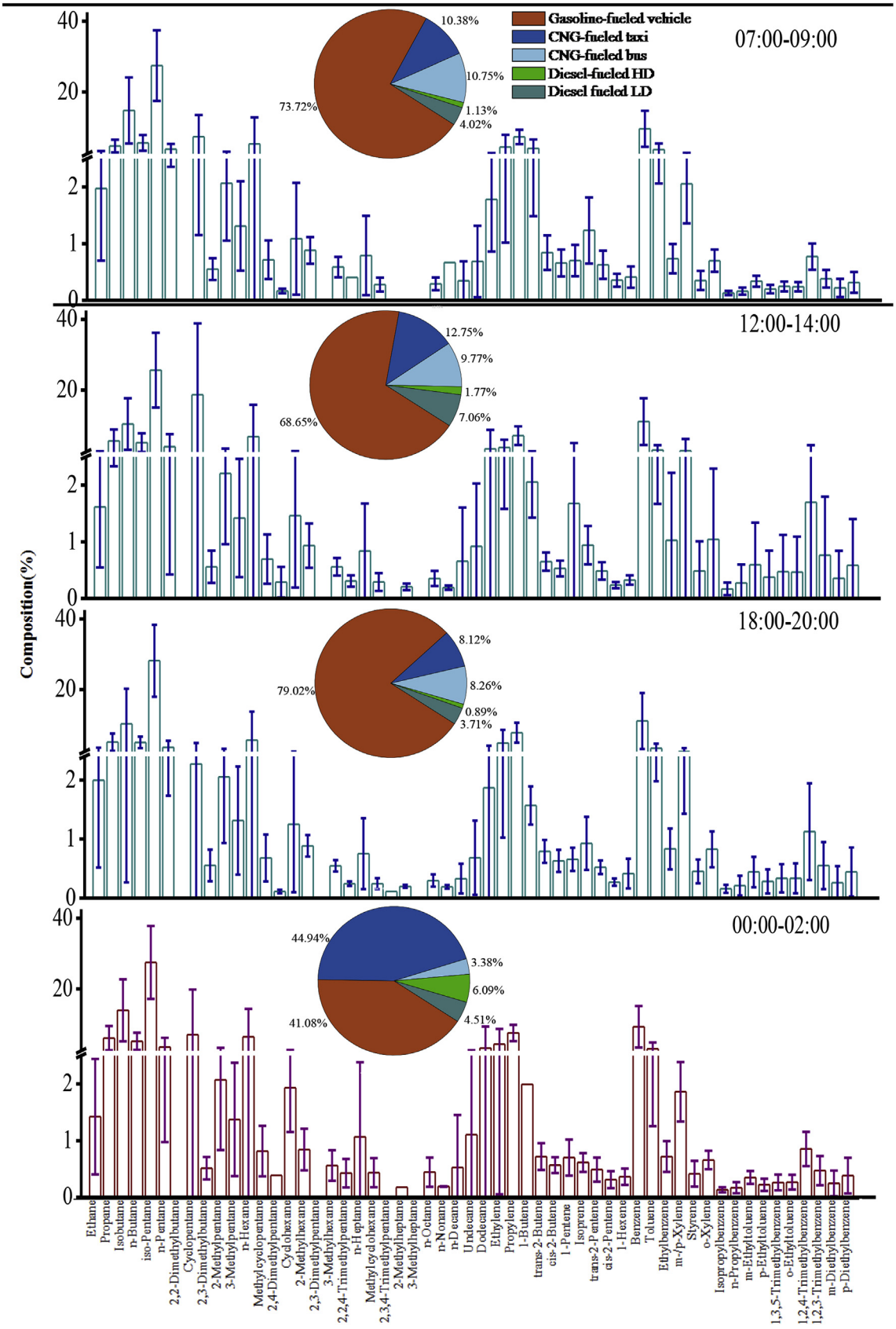

Fig. 2. $VOCs_{PAMS}$ composition and vehicle types in different time intervals.

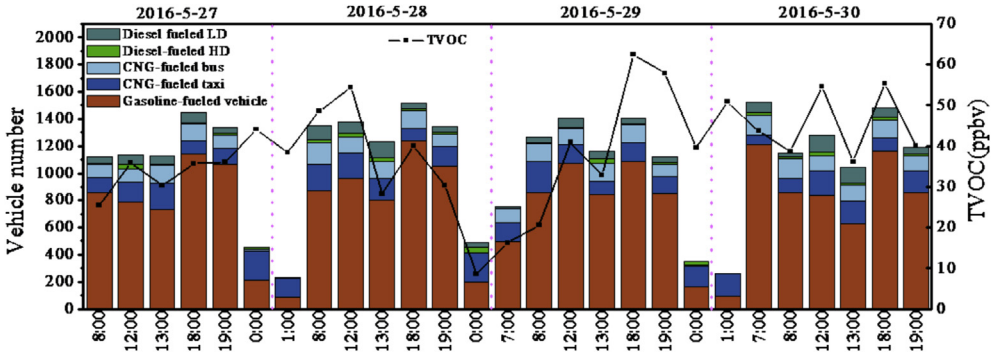

Fig. 3. The relationship between the $TVOC_{PAMS}$ and total vehicles number in a selective period.

particularly for the vehicles with worn and long millage-used engines in developing cities. Liu et al. (2008a) reported the source profiles of VE in China and a lower T/B ratio (<<1) was seen for diesel exhaust. In another emission profile study, the T/B ratio was 0.61 and 1.61 for diesel and gasoline exhausts (Lu et al., 2003). Rather than VE, benzene is mainly originated from biomass burning, whereas toluene can be emitted from a widespread pollution sources such as industrial emission and solvent usage (Zhang et al., 2012). However, the influences from other pollution sources to our exact roadside location must not be dominated. It should be noted that there were many factories such as shoes manufacturing, printing and chemical plants in Guangzhou and Nanjing (Liu et al., 2008b; Yuan et al., 2012), the levels of toluene might be elevated due to the baseline influence at the sampling sites.

Molar ratio of *m,p*-xylene/ethylbenzene (X/E) is a good indicator for "photochemical aging" in terms of the evident different photochemical reactivity between *m,p*-xylene (atmospheric lifetime of 3hr) and ethylbenzene (atmospheric lifetime of 8hr). Our X/E ratio of 2.73 is very consistent to 2.61 ± 0.30 measured at the roadside in Hong Kong (Huang et al., 2015). Fresh local emission can be indexed with a high X/E ratio of ~3.0 (Kuntasal et al., 2013). Our value is higher than those (1.18–2.12) recorded in other studies (Table 2), further demonstrating that the air parcel in the sampling site was much fresher and less influenced by photochemical activities and pollutant transportation.

3.6. Source apportionment

PMF receptor model was applied for source apportionment in this study. Three to seven factors had been tested and attempted with our sample data to obtain optimal PMF solution. Estimated as nm-p(n + m), theoretical Q value is an efficient parameter to indicate reasonable of the identified results, where n represents the number of species, m is designated as the number of samples, and p is the number of factors attributed by the model (Huang et al., 2015). We finally compared those examination results and considered that four-factor PMF solution is the best fit for further analysis, when the relevant Q value equals to 1672.0 in the robust-mode. With basic understanding on different potential VE impacted the air shed at the roadside and the corresponding maker species presented in the source profiles extracted by PMF receptor model, we assigned the four factors as gasoline fuel evaporation, gasoline fuel exhaust, CNG fuel consumption and diesel fuel consumption respectively (Table S2). Representative compounds were used to trace the emission sources. Factor 1 (F1) was characterized by high loadings of propylene, with abundant amounts of propane, *n*/*i*-butane and *n*/*i*-pentane which are generally associated with the emissions from CNG combustion (Turrio-Baldassarri et al., 2006; Hesterberg et al., 2008). Those taxis and public buses in Xi'an were CNG. FI is defined as CNG fuel consumption. The second factor (F2) was distinguished by high loading of *iso*-butane, *iso*-pentane, benzene, propane, *n*-butane and certain amounts of toluene. This series of compounds are highly correlated with the gasoline-related combustion, F2 is apportioned to gasoline fuel exhaust. High abundances of ethylene, *iso*-pentane, propylene, propane, undecane and dodecane were loaded in Factor3 (F3). Considering that these compounds are originated from diesel-fueled emission, F3 is identified as diesel fuel consumption. The last factor (F4) was dominated with *iso*-pentane and certain amounts of *iso*-butane, propylene, benzene and toluene. We defined F4 as gasoline fuel evaporation as the strong composition of *iso*-pentane.

Fig. 6 illustrates the contributions of the four sectors characterized by the PMF receptor model. The gasoline fuel evaporation is the largest contributors, accounting for 51.6% of to the $TVOC_{PAMS}$ at the roadside, which was about three times of the contribution from gasoline exhaust (17.1%). Frequent braking and idling of vehicles could promote more evaporation of the fuels at the sampling location (Ho et al., 2009), where is ~20 m away to the traffic lights. The contribution of CNG fuel consumption is 19.3%. In recent decade, the cleaner energy of CNG has been substituted with traditional fossil fuels to be widely used in public transportation in China because of its less pollutants emission and lower cost. Diesel fuel consumption contributed 12.0% to the $TVOC_{PAMS}$. Those PMF results were highly consistent with the vehicles compositions counted during the sampling period (refer to Fig. 6). It must be noted that emission factor (EF) of each vehicle type and stage of engine is the most critical factor in characterization of the VE and could be used to evidence the precision of source apportionment with those VE markers. However, there is currently a lack of any systematic EF database available in Xi'an or even in Northwest China. Our comparisons and interpretations are thus limited to the vehicle numbers.

3.7. Ozone formation potentials (OFPs)

To further understand the roles of vehicle exhaust in the formation of surface O_3, Ozone formation potential (OFP) were calculated based on the average mixing ratios and the maximum incremental reactivity coefficients (MIR) of $VOCs_{PAMS}$ quantified in the present study (Carter, 1994):

$$OFP_i = MIR_i \times C_i \quad (4)$$

where C_i, represents the mixing ratio (ppbv) for species *i*. The MIRs were obtained from Carter (1994).

Table 4 lists the top ten $VOCs_{PAMS}$ with the highest OFPs.

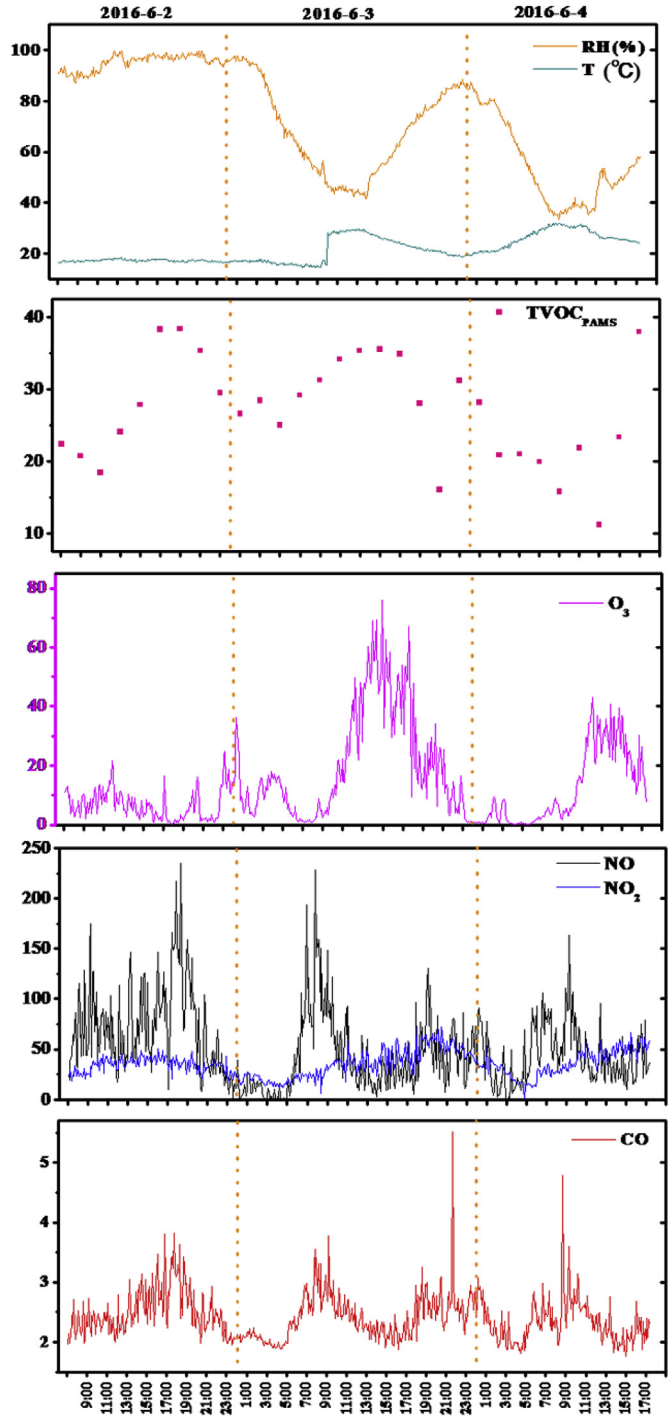

Fig. 4. Temporal variations of the meteorological parameters and mixing ratios of $TVOC_{PAMS}$ and trace gases during the strengthened sampling period.

Propylene had the highest value, followed by 1-butene, *iso*-pentane, ethylene, *m*-/*p*-xylene, cyclopentane, *iso*-butane, isoprene, toluene and *trans*-2-butene. Those compounds in different rank were consistent with the results from other relevant roadside studies. In this study, the first three largest contributors to OFP were all gasoline fuel consumptions related. This is highly reasonable as~70% of the vehicles were gasoline-fueled private cars during the sampling periods (Table 1). Meanwhile, the contributions from CNG fueled-vehicles should not be ignored due to high

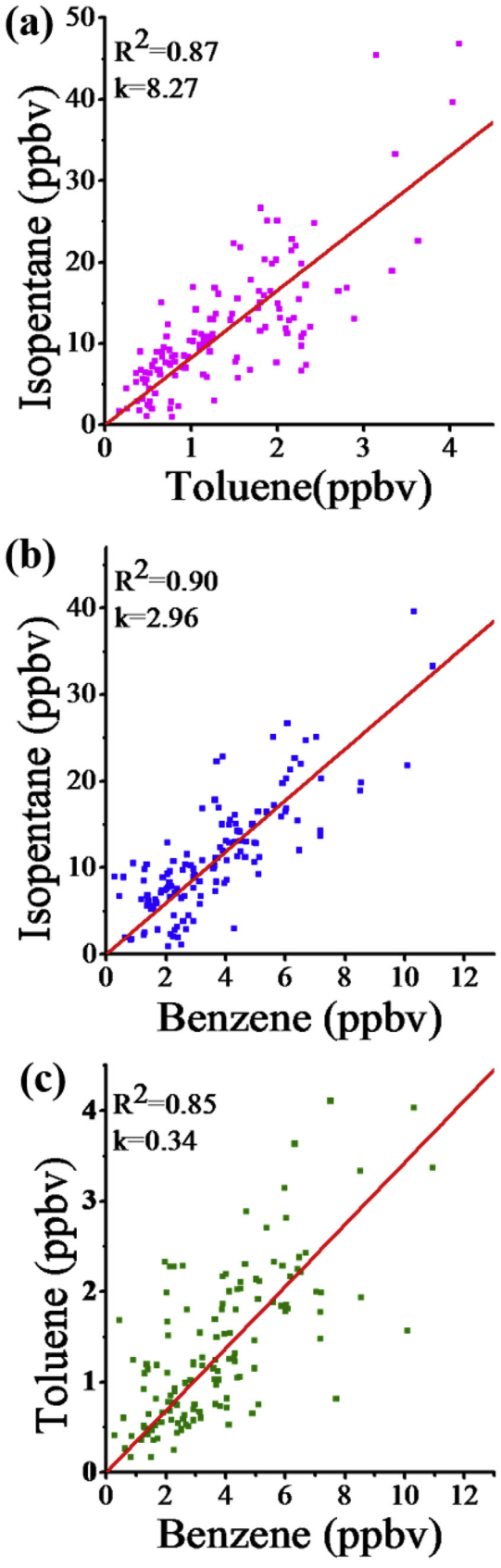

Fig. 5. Correlations of the mixing ratios between (a) *iso*-pentane and benzene; (b) *iso*-pentane and toluene; (c) benzene and toluene.

Table 3
Mixing ratios of BTEX(ppbv) and their molar ratios in different traffic-influenced sites.

Aromatics	Xi'an China 2016	Guangzhou China 2005	Nanjing China 2006–2007	Chang Chun China 1997–1998	Hong Kong China 2010–2011	Antwerp Belgium 2005
	This study	Tang et al., 2008	Wang and Zhao, 2008	Liu et al., 2000	Huang et al., 2015	Buczynska et al., 2009
Benzene	3.75 ± 2.31	2.07 ± 0.52	1.84 ± 1.09	11.06 ± 8.36	0.91 ± 0.09	0.72 ± 0.20
Toluene	1.31 ± 0.83	4.01 ± 2.34	4.82 ± 2.51	19.53 ± 8.45	2.74 ± 0.25	2.31 ± 0.78
Ethylbenzene	0.30 ± 0.17	0.91 ± 0.36	0.61 ± 0.44	3.97 ± 1.39	0.52 ± 0.07	0.34 ± 0.06
m,p-Xylene[a]	0.82 ± 0.50	1.92 ± 0.64	0.72 ± 0.59	4.94 ± 2.56	0.78 ± 0.11	0.72 ± 0.15
T/B[b]	0.36	1.93	2.62	1.77	3.03	3.22
B/E	12.50	2.27	3.02	2.79	1.75	2.12
T/E	4.37	4.41	7.90	4.92	5.27	6.79
X/E	2.73	2.11	1.18	1.24	1.50	2.12

[a] *m*-Xylene and *p*-xylene are co-eluted in the chromatographic separation.
[b] B: benzene; T: toluene; E: ethylbenzene; X: *m,p*-xylene.

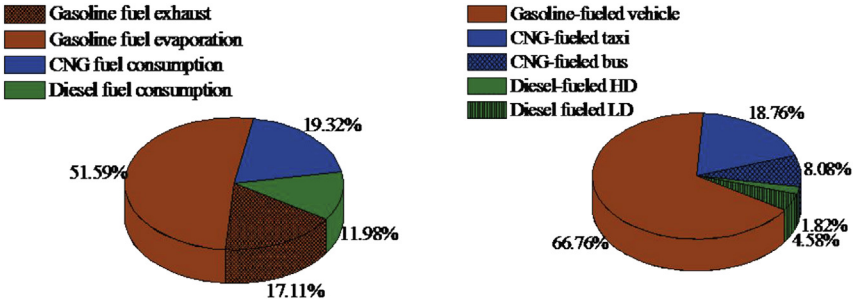

Fig. 6. Comparison of vehicle types contributions to the $VOCs_{PAMS}$ with PMF receptor model (left) and realistic traffic counts and classification (right).

Table 4
The top ten $VOCs_{PAMS}$ with the highest OFP at roadsides.

Xi'an China 2015 This study		Hong Kong China 2003 Ho et al., 2013		Jinan China 2010–2012 Liu et al., 2015		Tokyo Japan 2004 Hoshi et al., 2008	
Species	OFP	Species	OFP	Species	OFP	Species	OFP
Propylene	31.74	Ethylene	73.75	Propylene	17.35	Propylene	18.05
1-Butene	17.35	Propylene	24.22	cis-2-Butene	17.08	m, p-Xylene	14.39
iso-Pentane	16.05	n-Butane	7.53	Ethylene	12.43	Toluene	12.49
Ethylene	14.73	i-Butene	5.74	m,p-Xylene	8.57	1-Butene	8.19
m,p-Xylene[a]	12.11	2-Methyl-2-butene	6.75	Cyclopentane	5.81	Butane	4.73
Cyclopentane	11.55	Toluene	26.76	Isoprene	3.41	Iso-Pentane	4.08
Isobutane	9.31	m-Xylene	8.00	1-Butene	3.24	1,2,4-Trimethylbenzene	3.29
isoprene	4.51	o-Xylene	3.72	Toluene	2.85	Isobutane	3.27
Toluene	3.60	1,2,4-Trimethylbenzene	5.62	trans-2-Butene	2.80	trans-2-Butene	2.88
trans-2-Butene	3.56	1,2,3-Trimethylbenzene	2.96	o-Xylene	2.57	cis-2-Butene	2.52

[a] *m*-Xylene and *p*-xylene are co-eluted in the chromatographic separation.

OFP values from propylene and *iso*-butane (Besch et al., 2015; Singh et al., 2016). Currently there is still a lack of full source profiles for CNG or its combustion exhaust from the vehicle in China. More in-depth studies are thus needed to resolve the uncertainty since this energy source has been being promoted in use on either public vehicles or private cars. Diesel-fueled exhaust might be considered less impact on OFP, ascribed to lower mixing ratios and MIR of its markers such as the heavier alkanes and trimethylbenzenes (Liu et al., 2008a). The relatively lower OFP from the diesel exhaust might be also due to heavy-duty trucks are excluded to pass through the Second Ring Road from the traffic regulation in Xi'an.

4. Conclusion

This is the first comprehensive study on roadside VOCs conducted in Northwestern China. The maximum and minimum of $TVOC_{PAMS}$ were measured in the evening and night, respectively. The molar ratio of T/B in our study (0.36) is far lower than the range of 1.77–3.22 reported in other cities, potentially attributed to the strong contributions from the diesel emissions, particularly for the vehicles with worn and long millage-used engines in developing cities. The PMF results proved that the gasoline fuel consumption was the major contributor to roadside VOCs. Even though CNG was suggested to be a cleaner fuel than gasoline and diesel, its emission products of light species had much higher potentials in formation of surface O_3. More in-depth source characterization should be conducted in the future study, which could assist us to control the O_3 in China.

Acknowledgement

This research was financially supported by the National Key

Research and Development Program of China (2016YFA0203000),the National Science Foundation of China (41401567, 41503117, 41573138),and the Key Project of International Cooperation of the Chinese Academy of Sciences (GJHZ1543). Yu Huang is also supported by the "Hundred Talent Program" of the Chinese Academy of Sciences.

Appendix A. Supplementary data

Supplementary data related to this article can be found at http://dx.doi.org/10.1016/j.atmosenv.2017.04.029.

References

Andersson-Sköld, Y., Simpson, D., 2001. Secondary organic aerosol formation in northern Europe: a model study. J. Geophys. Res. Atmos. 106 (D7), 7357–7374.
Araizaga, A.E., Mancilla, Y., Mendoza, A., 2013. Volatile organic compound emissions from light-duty vehicles in Monterrey, Mexico: a tunnel study. Int. J. Environ. Res. 7 (2), 277–292.
Atkinson, R., 2000. Atmospheric chemistry of VOCs and NOx. Atmos. Environ. 34, 2063–2101.
Besch, M.C., Israel, J., Thiruvengadam, A., Kappanna, H., Carder, D., 2015. Emissions characterization from different technology heavy-duty engines retrofitted for CNG/diesel dual-fuel operation. SAE. Int. J. Engines 8 (3), 1342–1358.
Buczynska, A.J., Krata, A., Stranger, M., Locateli Godoi, A.F., Kontozova-Deutsch, V., Bencs, L., Naveau, I., Roekens, E., Van Grieken, R., 2009. Atmospheric BTEX-concentrations in an area with intensive street traffic. Atmos. Environ. 43 (2), 311–318.
Cao, Z., Yang, Y., Lu, J., Zhang, C., 2011. Atmospheric particle characterization, distribution, and deposition in Xi'an, Shaanxi Province, Central China. Environ. Pollut. 159 (2), 577–584.
Carter, W.P.L., 1994. Development of ozone reactivity scales for volatile organic compounds. J. Air Waste Manag. Assoc. 44, 881–899.
Chiang, H.-L., Tsai, J.-H., Chen, S.-Y., Lin, K.-H., Ma, S.-Y., 2007. VOC concentration profiles in an ozone non-attainment area: a case study in an urban and industrial complex metroplex in southern Taiwan. Atmos. Environ. 41 (9), 1848–1860.
Feng, T., Bei, N., Huang, R.-J., Cao, J., Zhang, Q., Zhou, W., Tie, X., Liu, S., Zhang, T., Su, X., Lei, W., Molina, L.T., Li, G., 2016. Summertime ozone formation in Xi'an and surrounding areas, China. Atmos. Chem. Phys. 16 (7), 4323–4342.
Finlayson-Pitts, B.J., Pitts, J.N., 1997. Tropospheric air pollution: ozone, airborne toxics, polycyclic aromatic hydrocarbons, and particles. Science 276 (5315), 1045–1051.
Guo, H., So, K.L., Simpson, I.J., Barletta, B., Meinardi, S., Blake, D.R., 2007. C1–C8 volatile organic compounds in the atmosphere of Hong Kong: overview of atmospheric processing and source apportionment. Atmos. Environ. 41 (7), 1456–1472.
Guo, H., Wang, T., Simpson, I.J., Blake, D.R., Yu, X.M., Kwok, Y.H., Li, Y.S., 2004. Source contributions to ambient VOCs and CO at a rural site in eastern China. Atmos. Environ. 38 (27), 4551–4560.
Han, M., Lu, X., Zhao, C., Ran, L., Han, S., 2015. Characterization and source apportionment of volatile organic compounds in urban and suburban Tianjin. China. Adv. Atmos. Sci. 32 (3), 439–444.
Hesterberg, T.W., Lapin, C.A., Bunn, W.B., 2008. A comparison of emissions from vehicles fueled with diesel or compressed natural gas. Environ. Sci. Technol. 42 (17), 6437–6445.
Ho, K.F., Ho, S.S.H., Lee, S.C., Louie, P.K.K., Cao, J., Deng, W., 2013. Volatile organic compounds in roadside environment of Hong Kong. Aerosol Air Qual. Res. 13, 1331–1347.
Ho, K.F., Lee, S.C., Ho, W.K., Blake, D.R., Cheng, Y., Li, Y.S., Ho, S.S.H., Fung, K., Louie, P.K.K., Park, D., 2009. Vehicular emission of volatile organic compounds (VOCs) from a tunnel study in Hong Kong. Atmos. Chem. Phys. 9, 7491–7504.
Ho, S.S.H., Chow, J.C., Watson, J.G., Wang, L., Qu, L., Dai, W., Huang, Y., Cao, J., 2017. Influences of relative humidities and temperatures on the collection of C2-C5 aliphatic hydrocarbons with multi-bed (Tenax TA, Carbograph 1TD, Carboxen 1003) sorbent tube method. Atmos. Environ. 151, 45–51.
Hoshi, J.-y., Amano, S., Sasaki, Y., Korenaga, T., 2008. Investigation and estimation of emission sources of 54 volatile organic compounds in ambient air in Tokyo. Atmos. Environ. 42 (10), 2383–2393.
Huang, R.J., Zhang, Y., Bozzetti, C., Ho, K.F., Cao, J.J., Han, Y., Daellenbach, K.R., Slowik, J.G., Platt, S.M., Canonaco, F., Zotter, P., Wolf, R., Pieber, S.M., Bruns, E.A., Crippa, M., Ciarelli, G., Piazzalunga, A., Schwikowski, M., Abbaszade, G., Schnelle-Kreis, J., Zimmermann, R., An, Z., Szidat, S., Baltensperger, U., El Haddad, I., Prevot, A.S., 2014. High secondary aerosol contribution to particulate pollution during haze events in China. Nature 514 (7521), 218–222.
Huang, Y., Ling, Z.H., Lee, S.C., Ho, S.S.H., Cao, J.J., Blake, D.R., Cheng, Y., Lai, S.C., Ho, K.F., Gao, Y., Cui, L., Louie, P.K.K., 2015. Characterization of volatile organic compounds at a roadside environment in Hong Kong: an investigation of influences after air pollution control strategies. Atmos. Environ. 122, 809–818.
Jenkin, M.E., Clemitshaw, K.C., 2000. Ozone and other secondary photochemical pollutants: chemical processes governing their formation in the planetary boundary layer. Atmos. Environ. 34, 2499–2527.
Kampa, M., Castanas, E., 2008. Human health effects of air pollution. Environ. Pollut. 151 (2), 362–367.
Kansal, A., 2009. Sources and reactivity of NMHCs and VOCs in the atmosphere: a review. J. Hazard Mater 166 (1), 17–26.
Knox, E.G., 2005. Childhood cancers and atmospheric carcinogens. J. Epidemiol. Commun. H. 59 (2), 101–105.
Kuntasal, Ö.O., Kılavuz, S.A., Karman, D., Wang, D., Tuncel, G., 2013. C5–C12 volatile organic compounds at roadside, residential, and background locations in Ankara, Turkey: temporal and spatial variations and sources. J. Air Waste Manag. Assoc. 63, 1148–1162.
Lai, C.H., Peng, Y.P., 2012. Volatile hydrocarbon emissions from vehicles and vertical ventilations in the Hsuehshan traffic tunnel. Taiwan. Environ. Monit. Assess. 184 (7), 4015–4028.
Li, G.H., 2016. Contents of Sulfur and Hydrocarbons in Commercial Available Gasoline and Diesel Oils Sold in China. University of Chinese Academy of Sciences, Guangzhou, China (in Chinese).
Li, J., Xie, S.D., Zeng, L.M., Li, L.Y., Li, Y.Q., Wu, R.R., 2015. Characterization of ambient volatile organic compounds and their sources in Beijing, before, during, and after Asia-Pacific Economic Cooperation China 2014. Atmos. Chem. Phys. 15 (14), 7945–7959.
Liu, C., Xu, Z., Du, Y., Guo, H., 2000. Analyses of volatile organic compounds concentrations and variation trends in the air of Changchun, the northeast of China. Atmos. Environ. 34, 4459–4466.
Liu, Y., Shao, M., Fu, L., Lu, S., Zeng, L., Tang, D., 2008a. Source profiles of volatile organic compounds (VOCs) measured in China: Part I. Atmos. Environ. 42 (25), 6247–6260.
Liu, Y., Shao, M., Lu, S., Chang, C.-C., Wang, J.-L., Fu, L., 2008b. Source apportionment of ambient volatile organic compounds in the Pearl River Delta, China: Part II. Atmos. Environ. 42 (25), 6261–6274.
Liu, Z., Li, N., Wang, N., 2015. Characterization and source identification of ambient VOCs in Jinan, China. Air Qual. Atmos. Hlth 9 (3), 285–291.
Lu, S., Bai, Y., Zhang, G., Ma, J., 2003. Study on the characteristics of vocs source profiles of vehicleexhaust and gasoline emission. Acta Sci. Nat. Univ. Pekin. 39 (4), 507–511 (in Chinese).
Lu, S., Liu, Y., Shao, M., Huang, S., 2007. Chemical speciation and anthropogenic sources of ambient volatile organic compounds (VOCs) during summer in Beijing, 2004. Front. Environ. Sci. En. 1 (2), 147–152.
Lyu, X.P., Chen, N., Guo, H., Zhang, W.H., Wang, N., Wang, Y., Liu, M., 2016. Ambient volatile organic compounds and their effect on ozone production in Wuhan, central China. Sci. Total Environ. 541, 200–209.
Miller, M.S., Friedlander, S.K., Hidy, G.M., 1972. A chemical element balance for the pasadena aerosol. J. Colloid. Interf. Sci. 39 (1), 165–176.
Miller, S.L., Anderson, M.J., Daly, E.P., Milford, J.B., 2002. Source apportionment of exposures to volatile organic compounds. I. Evaluation of receptor models using simulated exposure data. Atmos. Environ. 36, 3629–3641.
Ning, Z., Sioutas, C., 2010. Atmospheric processes influencing aerosols generated by combustion and the inference of their impact on public exposure: a review. Aerosol Air Qual. Res. 10, 43–58.
Paatero, P., 1997. Least squares formulation of robust non-negative factor analysis. Chemom. Intell. Lab. 37, 23–35.
Polissar, A.V., Hopke, P.K., Paatero, P., Malm, W.C., Sisler, J.F., 1998. Atmospheric aerosol over Alaska: 2. Elemental composition and sources. J. Geophys. Res. Atmos. 103 (D15), 19045–19057.
Shao, P., An, J., Xin, J., Wu, F., Wang, J., Ji, D., Wang, Y., 2016. Source apportionment of VOCs and the contribution to photochemical ozone formation during summer in the typical industrial area in the Yangtze River Delta, China. Atmos. Res. 176–177, 64–74.
Singh, S., Mishra, S., Mathai, R., Sehgal, A.K., Suresh, R., 2016. Comparative study of unregulated emissions on a heavy duty CNG engine using CNG &hydrogen blended CNG as fuels. SAE. Int. J. Engines 9 (4), 2202–2300.
Song, J., 2016. Major phases in the increment of vehicles. West China Dev. 8, 101–103 (in Chinese).
Tang, J.H., Chan, L.Y., Chan, C.Y., Li, Y.S., Chang, C.C., Wang, X.M., Zou, S.C., Barletta, B., Blake, D.R., Wu, D., 2008. Implications of changing urban and rural emissions on non-methane hydrocarbons in the Pearl River Delta region of China. Atmos. Environ. 42 (16), 3780–3794.
Tsai, W.Y., Chan, L.Y., Blake, D.R., Chu, K.W., 2006. Vehicular fuel composition and atmospheric emissions in South China: Hong Kong, Macau, Guangzhou, and Zhuhai. Atmos. Chem. Phys. 6, 3281–3288.
Turrio-Baldassarri, L., Battistelli, C.L., Conti, L., Crebelli, R., De Berardis, B., Iamiceli, A.L., Gambino, M., Iannaccone, S., 2006. Evaluation of emission toxicity of urban bus engines: compressed natural gas and comparison with liquid fuels. Sci. Total Environ. 355 (1–3), 64–77.
USEPA, 2008. EPA Positive Matrix Factorization (PMF) 3.0 Fundamentals & User Guide. USEPA Office of Research and Development.
Velasco, E., Lamb, B., Westberg, H., Allwine, E., Sosa, G., Arriaga-Colina, J.L., Jobson, B.T., Alexander, M.L., Prazeller, P., Knighton, W.B., Rogers, T.M., Grutter, M., Herndon, S.C., Kolb, C.E., Zavala, M., Foy, B.d., Volkamer, R., Molina, L.T., Molina, M.J., 2007. Distribution, magnitudes, reactivities, ratios and diurnal patterns of volatile organic compounds in the Valley of Mexico during the MCMA 2002 & 2003 field campaigns. Atmos. Chem. Phys. 7, 329–353.
Wang, H., Qiao, Y., Chen, C., Lu, J., Dai, H., Qiao, L., Lou, S., Huang, C., Li, L., Jing, S., Wu, J., 2014. Source profiles and chemical reactivity of volatile organic

compounds from solvent use in Shanghai. China. Aerosol Air Qual. Res. 14, 301–310.
Wang, J., Jin, L., Gao, J., Shi, J., Zhao, Y., Liu, S., Jin, T., Bai, Z., Wu, C.Y., 2013. Investigation of speciated VOC in gasoline vehicular exhaust under ECE and EUDC test cycles. Sci. Total Environ. 445–446, 110–116.
Wang, L.Q., Li, B.W., Huang, Y., Ho, S.S.H., Cao, J.J., Xue, Y.G., 2016. The monitoring and analysis methods of volatile organic compounds in the ambient air. J. Earth Environ. 7 (2), 130–139 (in Chinese).
Wang, M., Shao, M., Chen, W., Lu, S., Liu, Y., Yuan, B., Zhang, Q., Zhang, Q., Chang, C.C., Wang, B., Zeng, L., Hu, M., Yang, Y., Li, Y., 2015. Trends of non-methane hydrocarbons (NMHC) emissions in Beijing during 2002–2013. Atmos. Chem. Phys. 15 (3), 1489–1502.
Wang, P., Zhao, W., 2008. Assessment of ambient volatile organic compounds (VOCs) near major roads in urban Nanjing, China. Atmos. Res. 89, 289–297.
Wang, X., Shen, Z., Cao, J., Zhang, L., Liu, L., Li, J., Liu, S., Sun, Y., 2012a. Characteristics of surface ozone at an urban site of Xi'an in Northwest China. J. Environ. Monit. 14 (1), 116–126.
Wang, X., Sheng, G., Fu, J., Chan, C., Lee, S.C., Chan, L.Y., Wang, Z., 2002. Urban roadside aromatic hydrocarbons in three cities of the Pearl River Delta, People's Republic of China. Atmos. Environ. 36, 5141–5148.
Wang, Y., Ren, X., Ji, D., Zhang, J., Sun, J., Wu, F., 2012b. Characterization of volatile organic compounds in the urban area of Beijing from 2000 to 2007. J. Environ. Sci. 24 (1), 95–101.
Wu, F., Yu, Y., Sun, J., Zhang, J., Wang, J., Tang, G., Wang, Y., 2016a. Characteristics, source apportionment and reactivity of ambient volatile organic compounds at Dinghu Mountain in Guangdong Province, China. Sci. Total Environ. 548–549, 347–359.
Wu, R., Li, J., Hao, Y., Li, Y., Zeng, L., Xie, S., 2016b. Evolution process and sources of ambient volatile organic compounds during a severe haze event in Beijing, China. Sci. Total Environ. 560–561, 62–72.
Yuan, B., Chen, W., Shao, M., Wang, M., Lu, S., Wang, B., Liu, Y., Chang, C.-C., Wang, B., 2012. Measurements of ambient hydrocarbons and carbonyls in the Pearl River Delta (PRD). China. Atmos. Res. 116, 93–104.
Yun, W., 2015. The Influence of Using Motor Vehicle Alternative Fuel (Natural Gas) on $PM_{2.5}$ in Guanzhong Region and Abatement Analysis. Chang'an University, Xi'an, China (in Chinese).
Zhang, Y., Mu, Y., Liang, P., Xu, Z., Liu, J., Zhang, H., Wang, X., Gao, J., Wang, S., Chai, F., Mellouki, A., 2012. Atmospheric BTEX and carbonyls during summer seasons of 2008–2010 in Beijing. Atmos. Environ. 59, 186–191.
Ziemann, P.J., Atkinson, R., 2012. Kinetics, products, and mechanisms of secondary organic aerosol formation. Chem. Soc. Rev. 41 (19), 6582–6605.